Journal of Applied Polymer Science

Fabrication of Large-Scale Superhydrophobic Composite Films with Enhanced Tensile Properties by Multinozzle Conveyor Belt Electrospinning

Shuai Wang,[1,2] Yubo Yang,[1] Yang Zhang,[3] Xiaoliang Fei,[1] Chen Zhou,[1] Yue Zhang,[1] Yaoxian Li,[1] Qingbiao Yang,[1] Yan Song[4]

[1]Department of Chemistry, Jilin University, Changchun 130021, People's Republic of China
[2]College of Chemistry and Environmental Science, Inner Mongolia Normal University, Huhhot, 010022, People's Republic of China
[3]Inner Mongolia Engineering Research Center for Water-Saving Agriculture, Inner Mongolia Normal University, Huhhot, 010022, People's Republic of China
[4]Department of Chemical Engineering, Jilin Institute of Chemical Technology, Jilin, 132022, People's Republic of China
Correspondence to: Q. Yang or Y. Song (E-mail: yangqb@jlu.edu.cn or songyan199809@163.com)

ABSTRACT: Large-scale superhydrophobic composite films with enhanced tensile properties were prepared by multinozzle conveyor belt electrospinning. First, a strategy of conveyor belt electrospinning was introduced for large-scale fabrication since the conveyor belt can expand the electrospinning area unlimitedly. During the electrospinning (or electrospraying) process, certain kinds of fibers are combined on the conveyor belt in one electrospinning (or electrospraying) step. The superhydrophobicity of electrospun film can be achieved by the presence of PS beads and bead-on-string PVDF fibers, while submicron PAN fibers are responsible for the improvement of mechanical properties. The result shows that CA value of the surface comprising of PS beads and bead-on-string PVDF fibers could reach up to 155.0°. As the submicron PAN fibers increased, the value of CA decreased, changing from 155.0° to 140.0°, meanwhile the tensile strength of composite film was enhanced from 1.14 to 4.12 MPa correspondingly which is beneficial to putting the films into practice. © 2013 Wiley Periodicals, Inc. J. Appl. Polym. Sci. **2014**, *131*, 39735.

KEYWORDS: surfaces and interfaces; electrospinning; mechanical properties; porous materials

Received 6 January 2013; accepted 6 July 2013
DOI: 10.1002/app.39735

INTRODUCTION

Wettability is one of the important properties of a solid surface. A direct expression of the wettability of a surface is the contact angle (CA) of a water droplet on the surface. Superhydrophobic surfaces with a CA higher than 150°, very low hysteresis, and low surface free energy are becoming attractive in recent years due to their importance in fundamental research and their special properties such as anti-contamination, self-cleaning, and nonstick, which are widely used in industrial applications and daily life.[1,2]

Recent reports have revealed that the mechanism of this phenomenon proposes is related to a double roughness on their surface (nanostructures on microstructures) and low-surface-energy coatings,[3–5] where surface roughness is the key factor once the components of materials have been determined, since a hydrophilic material can produce surfaces with the CA larger than 150° after surface decoration.[6]

Numerous technologies and methods have been applied to fabricate superhydrophobic surfaces which include electrochemical deposition,[7,8] lithography,[9] chemical vapor deposition,[10] plasma etching,[11] phase separation,[12] sol–gel methods,[13] electrospinning (or electrospraying),[14–16] assembly,[17] array of nanotubes/nanofibers,[18,19] and solution-immersion methods.[20] However, most of them have certain drawbacks which prevent the further application such as complex processing, moreover, high cost and limitation in large-scale manufacture are some other aspects need consideration. Due to its ease of implementation, its low-cost, and its applicability to large-scale superhydrophobic surfaces, electrospinning (or electrospraying) has emerged as a promising and feasible method to produce surfaces with appropriate roughness and morphology.[21–23]

Electrospinning as a simple and versatile method has been applied for producing continuous fibers with diameters ranging from tens of nanometers to submicron scale. The polymer or composite fibers could be obtained by applying a high voltage to a viscous solution. Morphology, structure, and property of fibrous films could be controlled by adjusting the solution properties and processing parameters such as solution viscosities, temperature,[24,25] etc. Attracted by its simple process of production and the ease of controlling surface morphology by

varying electrospinning conditions, people attempt to integrate both the physical and chemical properties of electrospun mat to mimic the topography of the lotus leaf and to accomplish a high water CA.[26,27]

Polystyrene (PS), one of the most often used thermoplastic polymer, has been widely explored to fabricate superhydrophobic electrospun mat surfaces based on its low surface energy. To mimic the structure of lotus-leaf, several groups have succeeded in preparing porous composite films with a superhydrophobic surface via electrospraying a dilute PS solution. However, in reality, these electrosprayed composite microsphere/nanofiber films have their limits because of their mechanical unstability. The electrosprayed films are fragile. When a water droplet slides on this PS surface, some clusters of PS microspheres separates from the substrate spontaneously and floats on the water droplet. Moreover, the inadequacy of mechanical stability is also the restriction of preparing the large-scale superhydrophobic surfaces. To improve the mechanical stability of membranes, polyacrylonitrile (PAN), as a kind of perfect reinforcement material due to its strong intrachain and interchain interactions through secondary bonding,[28] could successfully competent for this job. Besides, PAN is an outstanding hydrophilic material and changing a hydrophilic material into a superhydrophobic material by modification or doping is a valuable research.

Poly (vinylidene fluoride) (PVDF) as a new unique material with extremely low surface energy has come out recently due to its flexibility and thermal stability. Besides, PVDF is an advanced material for film application due to its unique advantages such as good processability, excellent mechanical property, and exceptional chemical stability. Hence, PVDF film is widely used in structural material coating applications, such as certain surface materials of vehicle, boots, raincoat, and the cover of outdoor air conditioner,[29,30] etc. In recent years, several types of superhydrophobic surfaces, produced by electrospinning PVDF, have been reported in the literature.[31,32]

In this study, in order to fabricate large-scale superhydrophobic surfaces, a multinozzle conveyor belt electrospinning device is designed to place three (or more) nozzles on the top of the rolling conveyor belt (Figure 1). The first jet is charged with producing PS microspheres which play a key role in increasing the surface roughness of electrospun film. From the second nozzle, the bead-on-string PVDF is produced to construct the hierarchical microsphere/nanofiber structure and bind the PS microspheres tightly owing to the bead-on-string morphology. The last nozzle is responsible for introducing submicron-scale PAN fibers to further strengthen the mechanical stability of the film. It has been demonstrated experimentally that the precursor solutions in every nozzle have the same charge, and in the electrospinning (or electrospraying) process, the mutual Coulombic interactions between them influence the paths of individual electrified jets.[33,34] However, in our experiment, the distance between each nozzle is not particularly close. Therefore, with the rapid rolling of conveyor belt, three kinds of beads/fibers can be superimposed mixed easily. And, at the same time, large-scale fabrication is achieved which puts our device in advantageous position. The most obvious improvement in our design is that the collector is refitted into a conveyor belt, which makes the area of the electrospun mat to be any scale if you want. Recently needleless electrospinning setups have been reported to increase nanofiber production rate successfully,[35,36] but they are still challenging to electrospin multiform nanofibers with different properties and morphologies simultaneously using a needleless electrospinning spinneret. In our design, multinozzle can solve this problem effectively. Under the power of high voltage supply, different beads/fibers were ejected from their own nozzles and subsequently deposited on the collector with the rotation of conveyor belt. Therefore, electrospun film provided with multiple properties can be obtained.

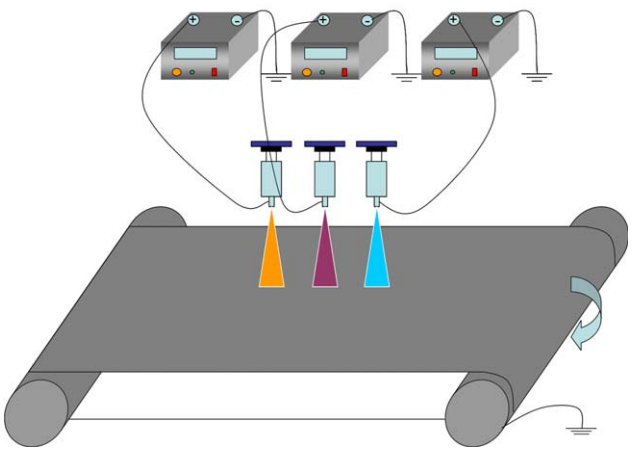

Figure 1. The schematic of the large-scale multinozzle electrospinning process. [Color figure can be viewed in the online issue, which is available at wileyonlinelibrary.com.]

Herein, a large-scale superhydrophobic film with enhanced tensile properties was prepared easily by multinozzle conveyor belt electrospinning. A developed multinozzle electrospining device of large-scale fabrication was designed successfully. We first significantly used the bead-on-string PVDF to construct the hierarchical microsphere/nanofiber structure which is similar to the surface of a lotus leaf and bind the PS microspheres tightly, resulting in a superhydrophobic surface. The surface of the composite mat exhibits a self-cleaning effect. To further reinforce the mechanical stability of PVDF/PS mats, PAN fibers were introduced into the mats via a multinozzle electrospinning process. The composition, superhydrophobicity, and mechanical properties of electrospun films can be well controlled by adjusting the weight ratio of various polymers. The weight ratio effect on the morphology and superhydrophobicity as well as the mechanical stability of the films is investigated in detail.

EXPERIMENTAL

Materials

Polystyrene (PS, M_w = 220,000) was purchased from Beijing Yanshan Chem. Poly (vinylidene fluoride) (PVDF, M_w = 400000–600000) was purchased from Shanghai Ofluorine Chemical Technology Co.. Polyacrylonitrile (PAN, M_w = 177,000) was purchased from CNPC Jilin Chemical. Dimethylformamide (DMF) was from Beijing Chemicals Co. China. All the materials were used without further purification.

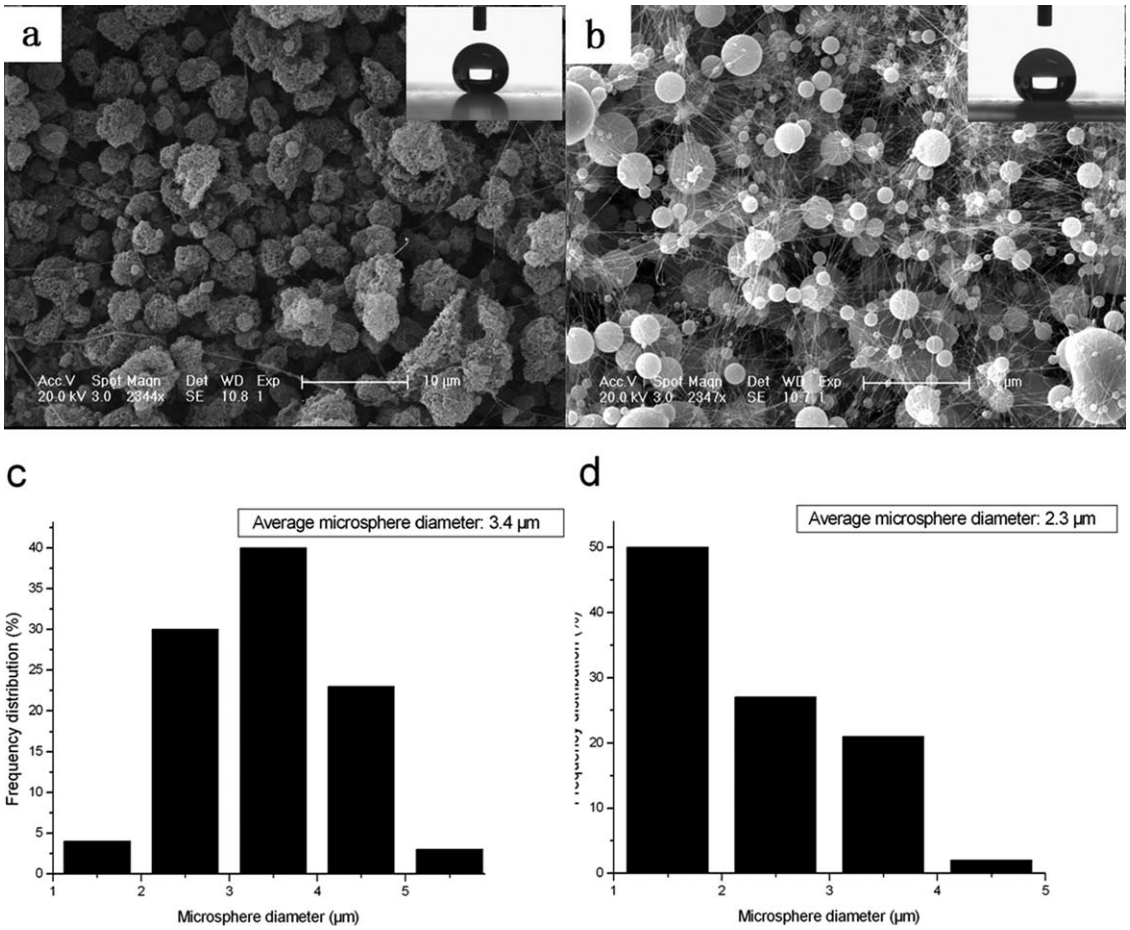

Figure 2. SEM images of electrosprayed mats prepared from (a) 4 wt % PS/DMF solution and (b) 21 wt % PVDF/DMF solution. The insets show the behavior of water droplets on their surfaces: (a) CA = 158.5°; (b) CA = 139.7°. Fiber diameter distributions of (c) PS and (d) PVDF.

Electrospinning (or Electrospraying)

PS solution with the concentration of 4 wt %, PVDF solution with the concentration of 21 wt % and PAN solution with the concentration of 12 wt % were prepared by dissolving certain amount of various polymers to DMF respectively. These precursor solutions were stirred for 12 h at room temperature to make each of the polymers dissolved completely. Each needle was connected to a high voltage supply which can generate positive DC voltages of up to 50 kV. The distance between the needle tip and the ground electrode was 15 cm. The applied positive voltages was 16 kV (PS) and 15 kV (PVDF and PAN). The feed rates of the precursor solutions were controlled by syringe pumps. Several groups of electrospun films with different weight ratios of microspheres/bead-on-string fibers/submicron-scale fibers were prepared. During electrospinning (or electrospraying), the applied electric field overcomes the surface tension of the polymeric solution, thereby ejecting a jet, which produces nanofibers (or microspheres) on the collector surface upon subsequent solvent evaporation and bending.

Characterization

An FEI XL30 scanning electron microscope was used to observe the morphologies of electrospun surfaces. The contact angles of the electrospun mats were measured with a drop shape analysis system (Krüss DSA100) in the sessile mode at room temperature. Stress–strain analysis was carried out at room temperature in a material testing station (Instron 5869) using standard procedures (ASTM standard 882 for thin films and membranes). Several specimens with lengths of 20 mm and widths of 10 mm were prepared for each tensile test.

RESULTS AND DISCUSSION

Surface Morphology and Surface Properties of Single PS Surface and Single PVDF Surface

PS and PVDF were usually used as superhydrophobic materials due to their low surface energy. In this study, PS film composed of sole particles was produced from a 4 wt % PS/DMF solution with enough roughness to form a CA of 158.5°. Figure 2(a) shows typical SEM picture of porous microspheres with morphology. The diameter of irregular microsphere ranges from 1 to 6 μm and the majority fall in the range of 2–5 μm [Figure 2(c)]. The surface of PS microspheres we produced was full of nanoholes so that each PS microsphere exhibited a well-developed micro/nano rough structure. The nanoholes on the surface of PS microspheres were gradually formed by a rapid phase separation during the electrospraying process. This bead structure and the porous and protuberant structure combined contributed to the roughness of PS mat. These nanoholes and

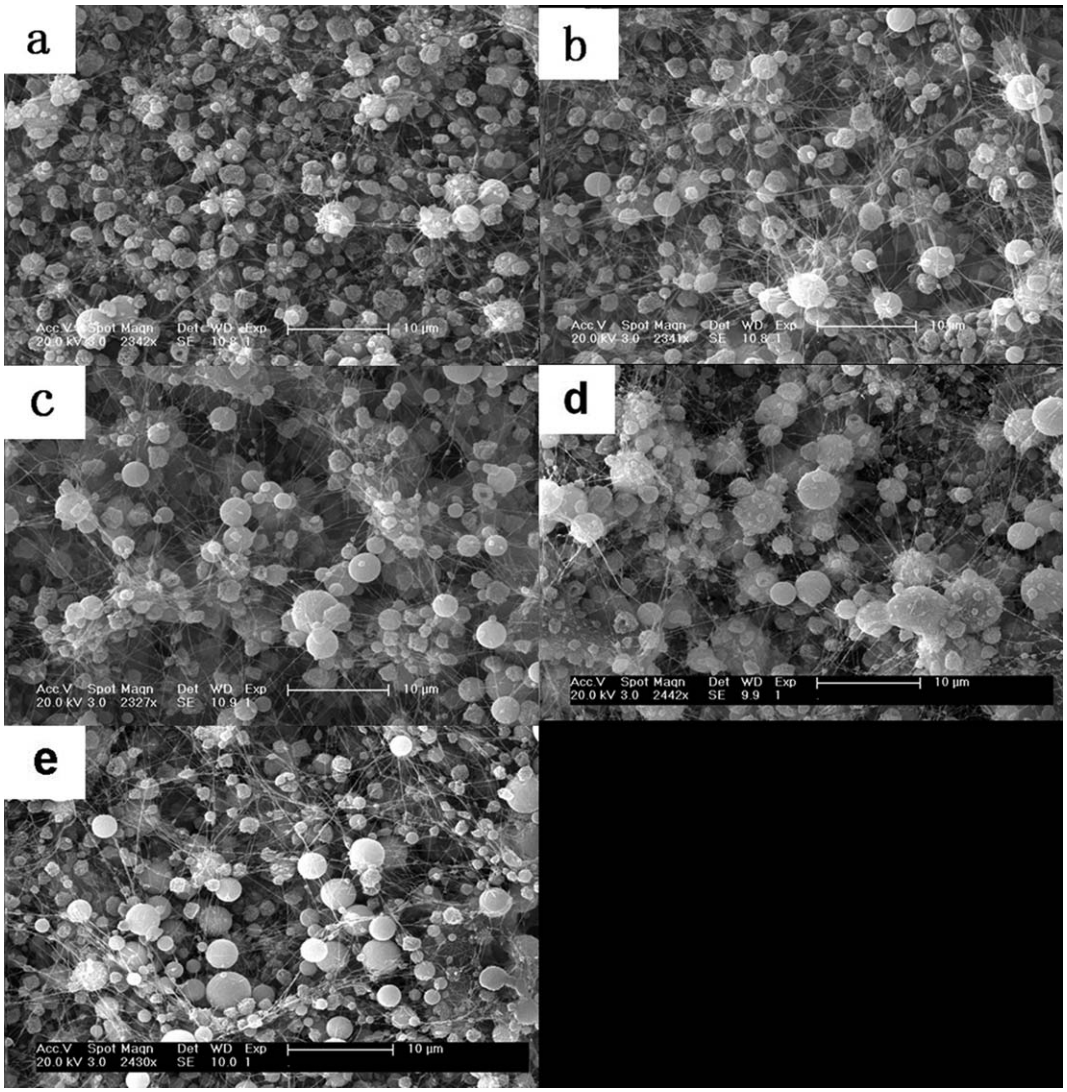

Figure 3. SEM images of electrosprayed composite films comprised of the weight ratio of PVDF/PS: (a) 1.73 : 1, (b) 2.60 : 1, (c) 3.47 : 1, (d) 4.33 : 1, and (e) 5.20 : 1.

the porous among PS microspheres can be seen as the grooves that assume the responsibility of trapping air. So they can efficiently reduce the actual contact area between the surface and water droplet, which makes this type of structure exhibit strong hydrophobicity. The Cassie–Baxter model[37] relates the surface wettability to the surface roughness

$$\cos\theta_{CB} = f_1 \cos\theta_S - f_2 \quad (1)$$

where f_1 and f_2 ($= 1 - f_1$) are the fractions of solid-water and air-water contact areas, respectively, and θ_S and θ_{CB} denote the apparent contact angles of a water droplet on a smooth surface and a rough surface composed of a solid and air, respectively. Given the CA of the flat PS film (96.6°) and the rough PS mats (158.5°), f_{PS} was calculated to be 7.86%, which indicated that the achievement of superhydrophobicity of PS mats was mainly a result of the air trapped in the nanoholes on the suface of PS microspheres and the porous characteristic among PS microspheres of mats. On our electrosprayed PS surface, the water droplet slides easily and moves in random directions even when PS films are slightly tilted. It could be explained that the irregular nanometer-scaled pores on the surface of beads and this porous and protuberant structure presented in our research are able to effectively trap sufficient air, creating a long and discontinuous contact line. However, when a water droplet slides on this PS surface, some clusters of PS microspheres separates from the substrate spontaneously and floats on the water droplet because the density of porous microspheres is lower than that of water. This drawback prevents its further application.

Accordingly, a stable superhydrophobic film, on which the PS microspheres cannot be taken away by the water droplet, should be prepared. Here we introduced bead-on-string PVDF to bind the PS microspheres tightly, and significantly, the bead-on-string PVDF could maintain the superhydrophobicity. The bead-on-string PVDF film as shown in Figure 2(b) was produced from a 21 wt % PVDF/DMF solution with some roughness to form a CA of 139.7°. The diameters of PVDF microspheres range from 1 to 5 μm and the majority are in the

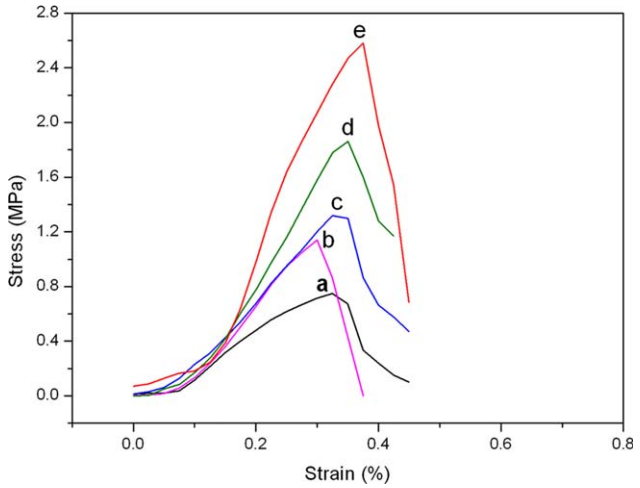

Figure 4. Stress–strain behavior of composite films formed with various weight ratios of PVDF/PS: (a) 1.73 : 1, 0.75 MPa, (b) 2.60 : 1, 1.14 MPa, (c) 3.47 : 1, 1.32 MPa, (d) 4.33 : 1, 1.86 MPa, and (e) 5.20 : 1, 2.58 MPa. [Color figure can be viewed in the online issue, which is available at wileyonlinelibrary.com.]

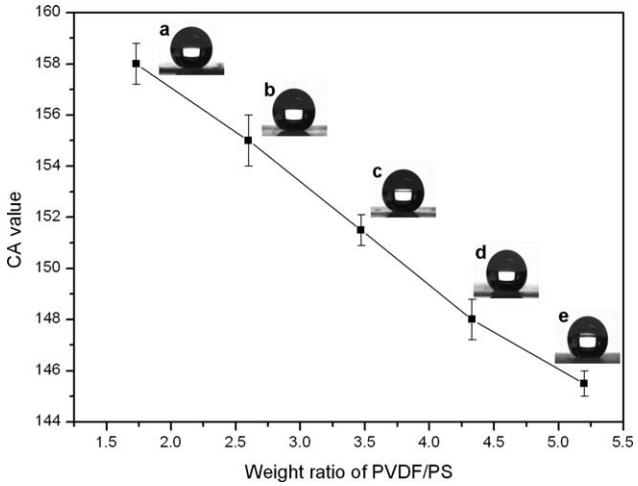

Figure 5. Variation of CA value of composite films based on different weight ratios of PVDF/PS: (a) 1.73 : 1, CA = 158.0 ± 0.8°, (b) 2.60 : 1, CA = 155.0 ± 1.0°, (c) 3.47 : 1, CA = 151.5 ± 0.6°, (d) 4.33 : 1, CA = 148.0 ± 0.8°, and (e) 5.20 : 1, CA = 145.5 ± 0.5°.

range of 1–3 μm [Figure 2(d)]. As shown in Figure 2(b), PVDF nanofibers and PVDF microspheres are interlaced closely, that was believed to bind the PS microspheres effectively.

Controllable Surface Morphology and Film Properties of PVDF/PS Composite Films

Composite films comprised of 21% PVDF solution and 4% PS solution were prepared by two-nozzle electrospraying, the weight ratios of bead-on-string PVDF fibers/PS microspheres varied from 1.73 : 1 to 5.20 : 1. Figure 3 presents the SEM images of composite mats formed with various weight ratios of PVDF/PS. As shown in Figure 3, two types of fibers (or microspheres) were mixed uniformly during the electrospraying. The introduced bead-on-string PVDF fibers successfully afford the role of supporting the whole film as the frame. It can be found that with the increased weight ratio of fibers from 21% PVDF solution, the film demonstrates an enhanced tensile strength (Figure 4). Because increasing syringe-pump flow rate of PVDF can stimulate the PVDF filaments get thicker and larger amount, which are beneficial to enhance the mechanical properties. However, as the quantity of bead-on-string PVDF fibers increases in the prepared film, the CA value of the surfaces tends to decline from 158.0° at a ratio of 1.73 : 1 to 145.5° when the ratio up to 5.20 : 1 (Figure 5). Given the CA of the flat PVDF film (100.2°) and the rough PVDF mats (139.7°), f_{PVDF} was calculated to be 28.84% according to eq. (1). f_{PS} is 7.86% that was calculated previously. It can be deduced that the morphology of electrosprayed 4% PS surface is rougher than the morphology of electrosprayed 21% PVDF surface. Therefore, the air trapped in the composite surface declined continuously when PVDF was introduced. As the weight ratio of bead-on-string PVDF fibers goes up, the amount of PS microspheres exposed on the surface of the composite film decreased sharply so that the surface roughness declined gradually and tended to the roughness of bead-on-string PVDF. As a result, the capability of preventing the surface being wetted by trapped air would decrease, making the apparent contact angle θ_{CB} decrease as described by Cassie–Baxter model. When the weight of bead-on-string PVDF fibers is 4.33 times as big as PS microspheres, affording a CA value of 148.0° < 150° as showed in Figure 5, the film cannot still be categorized as superhydrophobic films.

To further verify the effect of binding PS microspheres, the composite films were tested underwater. We put the various electrosprayed surfaces in water for 48 h to observe the changes of their weight. Remaining percentage of composite films formed with various weight ratios of PVDF/PS is showed in Figure 6. When bead-on-string PVDF was absent, the weight of PS film decreased a lot and left 70% only. When PVDF was introduced, the bead-on-string fibers effectively prevented the reduction in weight obviously. It can be proved that when the weight ratio rises up to 2.60 : 1, there was very little reduction in the weight of the composite films we prepared. Thus when

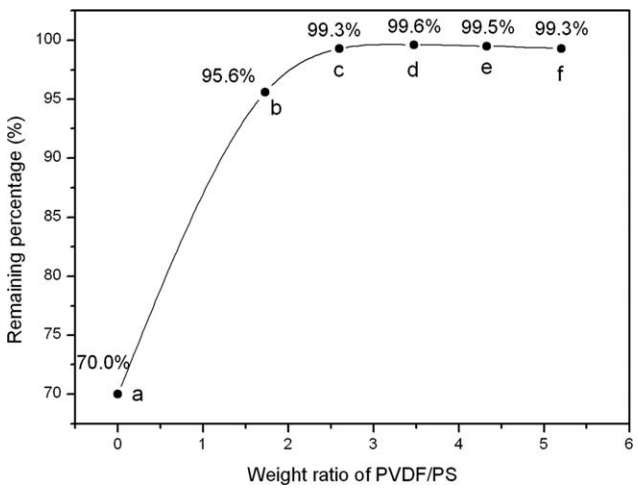

Figure 6. Remaining percentage of composite films formed with various weight ratios of PVDF/PS: (a) 0 : 1, (b) 1.73 : 1, (c) 2.60 : 1, (d) 3.47 : 1, (e) 4.33 : 1, and (f) 5.20 : 1.

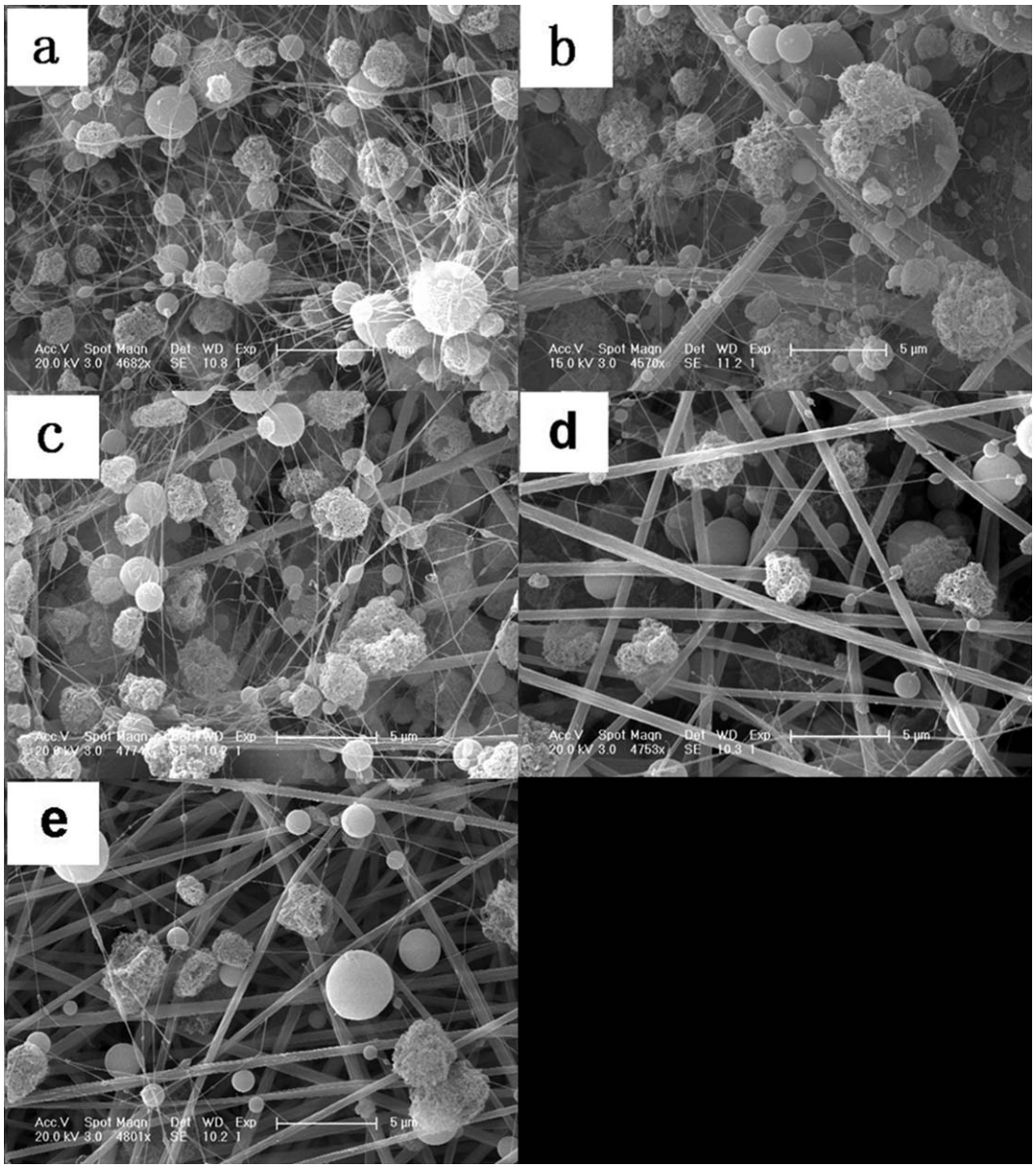

Figure 7. SEM images of electrospun composite films comprised of the weight ratio of PAN/PVDF/PS: (a) 0 : 2.60 : 1, (b) 0.30 : 2.60 : 1, (c) 0.60 : 2.60 : 1, (d) 0.90 : 2.60 : 1, (e) 1.20 : 2.60 : 1.

the weight ratio is higher than 2.60 : 1, the introduced bead-on-string PVDF fibers could successfully afford the role of binding the PS microspheres tightly.

Different Morphologies, Superhydrophobicity, and Mechanical Properties of PAN/PVDF/PS Composite Films Prepared by Conveyor Belt Electrospinning

Superhydrophobic surfaces were prepared desirably, nevertheless the films can break easily in practice because of the unstable frames which are made of bead-on-string PVDF fibers, and their scale constraint is another issue in use. Confronted with these situations, we actively made some changes with the films. To make the frame more stable, submicron-scale PAN fibers were further introduced to the bead-on-string film by the technique of multinozzle electrospinning, and at the same time achieved the effect of large-scale production. Different kinds of fibers interweave densely on the collector. The advantages of the new electrospinning device involved the possibility of enhancing the intensity of electrospun film by introducing large diameter fibers, the ease of adjusting the thickness and the proportion of different fibers depending on specific demand, and remarkably, preparing large-scale composite films.

Composite films comprised of 12% PAN solution, 21% PVDF solution, and 4% PS solution were prepared, the weight ratios of PAN fibers/bead-on-string PVDF fibers/PS microspheres varied from 0 : 2.60 : 1 to 1.20 : 2.60 : 1. (PAN is an outstanding hydrophilic material. There will be definitely a significant reduction in the superhydrophobicity of the composite electrospun films when PAN is introduced. So we decided to select a high superhydrophobic weight ratio of PVDF/PS mat by two-nozzle electrosprayed for preparation. However, when the weight ratio

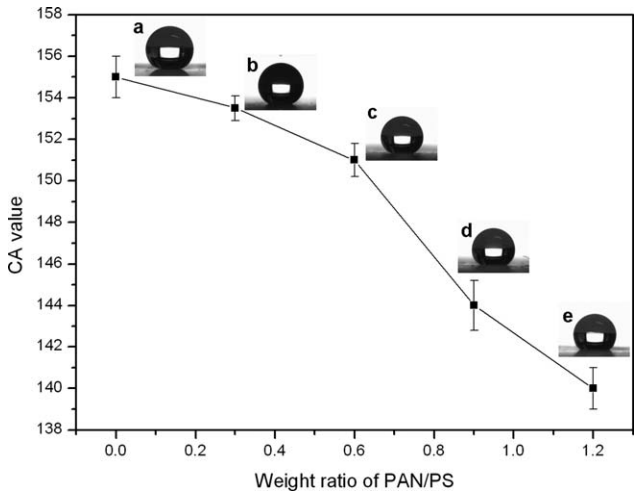

Figure 8. Variation of CA value of composite films based on different weight ratios of PAN/PVDF/PS: (a) 0 : 2.60 : 1, CA = 155.0 ± 1.0°, (b) 0.30 : 2.60 : 1, CA = 153.5 ± 0.6°, (c) 0.60 : 2.60 : 1, CA = 151.0 ± 0.8°, (d) 0.90 : 2.60 : 1, CA = 144.0 ± 1.2°, and (e) 1.20 : 2.60 : 1, CA = 140.0 ± 1.0°.

of bead-on-string PVDF fibers/PS microspheres is lower than 2.60 : 1, bead-on-string PVDF fibers could not effectively bind the PS microspheres tightly. Accordingly, we set 2.60 : 1 as a constant weight ratio of PVDF/PS. The SEM images in Figure 7 further confirm that three types of fibers were mixed uniformly during the electrospinning. PAN, PVDF, and PS fibers in our composite films were easily distinguished because of their obvious morphology distinction. The introduced PAN fibers with diameters ranging from 0.5 to 0.95 μm afford the role of supporting the whole film as the frame successfully. It could also be found that with the increased weight ratio of fibers from 12% PAN solution, the CA value of the surfaces tends to decline from 155.0° at a ratio of 0 : 2.60 : 1 to 140.0° when the ratio rises up to 1.20 : 2.60 : 1, because large diameter PAN fibers are not only hydrophilic, but also not favorable to increase the roughness and subsequently to form superhydrophobic surface. Additionally, increasing the syringe-pump flow rate of PAN can stimulate the PAN fibers get thicker and more, which is a disadvantage of making the surface hydrophobic. As a result, the hydrophobicity of the composite surfaces goes opposite when the PAN component in the films increases. The weight ratio of 0.60/2.60/1 (PAN/PVDF/PS) was a critical ratio as showed in Figure 8. The composite films lost their superhydrophobicity when the ratio was higher than 0.60/2.60/1.

The CA hysteresis is an important factor in determining surface hydrophobicity as well as the static CA. To make a surface superhydrophobic and water-repellent, the water CA should be high enough (>150°) and, more importantly, the CA hysteresis should be very small, so as to lead to a small roll-off angle of the water droplet. Sliding behavior of a water droplet is very crucial in evaluating the contact angle hysteresis. If a water droplet falls on the rough surface, there will be lots of cavities as the air pockets between the water droplet and the solid surface. When this water droplet slides on the superhydrophobic surface, there will be a transition from the Wenzel model[38] to the Cassie–Baxter model, as the Cassie-Baxter model describes that, as surface roughness factor keep increasing and passes a critical standard, the water receding angle increases noticeably at the same time (water does not penetrate into the surface cavity), thus minimizing the CA hysteresis. In our work, the SA of the electrospun composite films was tested using a 10 μL water droplet on their surfaces. When PAN was not introduced into the membrane (the weight ratios of PAN/PVDF/PS is 0 : 2.60 : 1), the SA is 3.8° so the water droplet could slide easily and move in random directions on our electrospun surface. The SA of the composite surfaces increased gradually as the weight ratios of PAN/PVDF/PS increase. When the weight ratio was 1.20 : 2.60 : 1, the water droplet could not slide anyway and adheres on the surface of the mat, thus leading to a large CA hysteresis apparently. Because PAN fibers are so hydrophile that water droplet cannot roll easily on the surface of the composite film if the film is full of PAN, and make the surface roughness decrease extremely. On the other hand, submicron-scale PAN fibers tend to advance three-phase contact line and make the three-phase line get continuous since a discontinuous and distorted three-phase contact line is apt to present a small CA hysteresis.[39] Therefore, as PAN fibers increased gradually, it is more and more difficult to keep water droplet rolling on the surface of the composite films.

The tensile properties of electrospun composite films were characterized. All of the electrospun mats were easily removed from substrate. Stress–strain behavior of composite films formed with various weight ratios of PAN/PVDF/PS is shown in Figure 9. The testing result shows that the mechanical properties of electrospun films benefit a lot from the presence of PAN fibers. The mechanical behavior of electrospun composite films depends on the properties of the blend components, the structure of various fibers, and the interaction between each polymer fiber. When the weight ratio of PAN fibers/bead-on-string PVDF fibers/PS

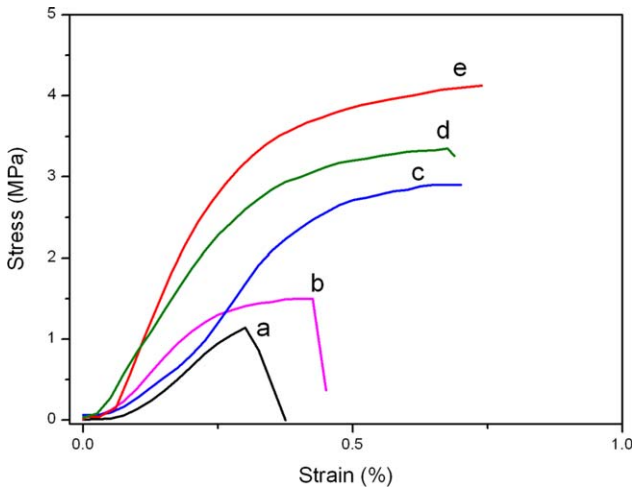

Figure 9. Stress–strain behavior of composite films formed with various weight ratios of PVDF/PS: (a) 0 : 2.60 : 1, 1.14 MPa, (b) 0.30 : 2.60 : 1, 1.50 MPa, (c) 0.60 : 2.60 : 1, 2.90 MPa, (d) 0.90 : 2.60 : 1, 3.35 MPa, and (e) 1.20 : 2.60 : 1, 4.12 MPa. [Color figure can be viewed in the online issue, which is available at wileyonlinelibrary.com.]

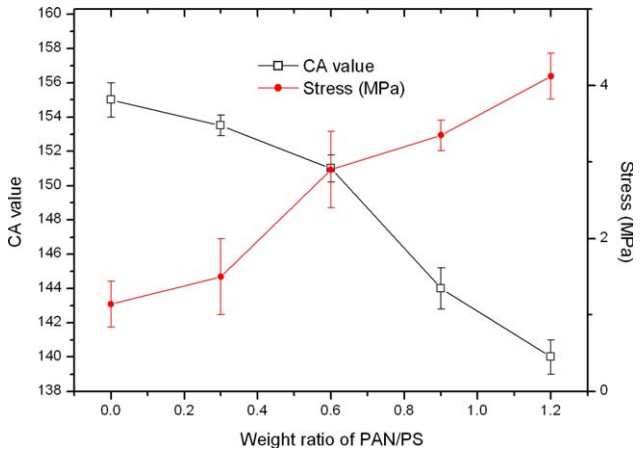

Figure 10. Variation of CA value and stress of composite films based on different weight ratios of PAN/PS. [Color figure can be viewed in the online issue, which is available at wileyonlinelibrary.com.]

microspheres varied from 0 : 2.60 : 1 to 1.20 : 2.60 : 1, not only the amount of PAN fibers increases, but also the diameter of PAN fibers gets a little bigger. As a result, the film demonstrates an enhanced tensile strength from 1.14 to 4.12 MPa. In the electrospinning (or electrospraying) process, three types of fibers could stick together firmly owing to the adhesion force of PAN fibers and the structure of PVDF bead-on-string fibers could prevent PAN fibers from moving when the electrospun films were elongated, so as to achieve the purpose of reducing the elongation. In addition, when the composite material is stretched, the PAN fibers which are parallel with the external force exhibit more effect of the excellent flexible and tensile characteristics, and the other PAN fibers will be affected by structure of PVDF bead-on-string fibers more. This dual effects lead to the mechanical stability enhancement of the composite material. Consequently, the mechanical properties of composite films were significantly enhanced by the increase of the content of PAN fibers. Figure 10 can clearly explain the changes of CA value and tensile strength of electrospun mat brought by the various weight ratios of three kinds of components. We take advantage of all of them, and then integrate their unique merits together into one prepared mat through electrospinning (or electrospraying). When the roughness of mat is maintained, PAN fibers also play an important role in improving the mechanical property of electrospun membrane. In this way, a large-scale superhydrophobic surface with mechanical integrity could be obtained.

CONCLUSIONS

In our research, large-scale superhydrophobic composite films with enhanced tensile properties were successfully fabricated through the blending of porous PS microspheres, bead-on-string PVDF fibers and PAN fibers via an advanced conveyor belt electrospining device. Large-scale fabrication without limit puts our conveyor belt electrospining device in advantageous position. During the electrospining (or electrospraying) process, three types of fibers were mixed easily. The simultaneous presence of PS microspheres, bead-on-string PVDF fibers afford the role of increasing surface roughness so that the composite film exhibits a superhydrophobic surface. The later introduced large diameter PAN fibers significantly improve the mechanical properties of electrospun sheet owing to the special character of PAN. The superhydrophobicity and the mechanical properties of electrospun composite film could be regulated by altering the weight ratio of PS microspheres/bead-on-string PVDF fibers/PAN fibers. We believe that this advanced electrospining device can be further explored to prepare more multifunctional materials with versatile properties desired in the future by mixing various substances uniformly.

ACKNOWLEDGEMENT

The authors gratefully acknowledge the support of the National Natural Science Foundation of China (No. 20874033).

REFERENCES

1. Zielecka, M.; Bujnowska, E. *Prog. Org. Coat.* **2006**, *55*, 160.
2. Kako, T.; Nakajima, A.; Irie, H.; Kato, Z.; Uematsu, K.; Watanabe, T.; Hashimoto, K. *J. Mater. Sci.* **2004**, *39*, 547.
3. Jiang, L.; Wang, R.; Yang, B.; Li, T. J.; Trigk, D. A.; Fujishima, A.; Hashimoto, K.; Zhu, D. B. *Pure Appl. Chem.* **2000**, *72*, 73.
4. Feng, L.; Li, S. H.; Li, Y. S.; Li, H. J.; Zhang, L. J.; Zhai, J.; Song, Y. L.; Liu, B. Q.; Jiang, L.; Zhu, D. B. *Adv. Mater.* **2002**, *14*, 1857.
5. Sun, T. L.; Feng, L.; Gao, X. F.; Jiang, L. *Acc. Chem. Res.* **2005**, *38*, 644.
6. Guo, C. W.; Feng, L.; Zhai, J.; Wang, G.. J.; Song, Y. L.; Jiang, L. *Chem. Phys. Chem.* **2004**, *5*, 750.
7. Chen, Z.; Li, F.; Hao, L. M.; Chen, A. Q.; Kong, Y. C. *Appl. Surf. Sci.* **2011**, *258*, 1395.
8. Bok, H. M.; Kim, S.; Yoo, S. H.; Kim, S. K.; Park, S. *Langmuir* **2008**, *24*, 4168.
9. Feng, J. S.; Tuominen, M. T.; Rothstein, J. P. *Adv. Funct. Mater.* **2011**, *21*, 3715.
10. Liu, H.; Feng, L.; Zhai, J.; Jiang, L.; Zhu, D. B. *Langmuir* **2004**, *20*, 5659.
11. Mundo, R. D.; Palumbo, F.; d'Agostino, R. *Langmuir* **2008**, *24*, 5044.
12. Han, J. T.; Xu, X. R.; Cho, K. W. *Langmuir* **2005**, *21*, 6662.
13. Wang, S. L.; Liu, C. Y.; Liu, G. C.; Zhang, M.; Li, J.; Wang, C. Y. *Appl. Surf. Sci.* **2011**, *258*, 806.
14. Wang, X. F.; Ding, B.; Yu, J. Y.; Wang, M. R. *Nano Today* **2011**, *6*, 510.
15. Guo, Y. D.; Tang, D. Y.; Gong, Z. L. *J. Phys. Chem. C* **2012**, *116*, 26284.
16. Ochanda, F. O.; Samaha, M. A.; Tafreshi, H. V.; Tepper, G. C.; Gad-el-Hak, M. *J. Appl. Polym. Sci.* **2012**, *123*, 1112.
17. Shi, F.; Wang, Z. Q.; Zhang, X. *Adv. Mater.* **2005**, *17*, 1005.
18. Sun, T. L.; Wang, G. J.; Liu, H.; Feng, L.; Jiang, L.; Zhu, D. B. *J. Am. Chem. Soc.* **2003**, *125*, 14996.

19. Feng, L.; Song, Y. L.; Zhai, J.; Liu, B. Q.; Xu, J.; Jiang, L.; Zhu, D. B. *Angew. Chem. Int. Ed.* **2003**, *42*, 800.
20. Zhu, X. T.; Zhang, Z. Z.; Men, X. H.; Yang, J.; Xu, X. H. *ACS Appl. Mater. Interfaces* **2010**, *2*, 3636.
21. Lee, M. W.; An, S.; Joshi, B.; Latthe, S. S.; Yoon, S. S. *ACS Appl. Mater. Interfaces* **2013**, *5*, 1232.
22. Nuraje, N.; Khan, W. S.; Lei, Y.; Ceylan, M.; Asmatulu, R. *J. Mater. Chem. A* **2013**, *1*, 1929.
23. Asmatulu, R.; Ceylan, M.; Nuraje, N. *Langmuir* **2011**, *27*, 504.
24. Li, Z.; Zhang, H. N.; Zheng, W.; Wang, W.; Huang, H. M.; Wang, C.; MacDiarmid, A. G.; Wei, Y. *J. Am. Chem. Soc.* **2008**, *130*, 5036.
25. Wang, L.; Topham, P. D.; Mykhaylyk, O. O.; Howse, J.; Bras, W.; Jones, R. A.; Ryan, A. J. *Adv. Mater.* **2007**, *19*, 3544.
26. Jiang, L.; Zhao, Y.; Zhai, J. *Angew. Chem.* **2004**, *116*, 4438.
27. Acatay, K.; Simsek, E.; Ow-Yang, C.; Menceloglu, Y. Z. *Angew. Chem.* **2004**, *116*, 5322.
28. Esrafilzadeh, D.; Jalili, R.; Morshed, M. *J. Appl. Polym. Sci.* **2008**, *110*, 3014.
29. Naoya, Y.; Masao, T.; Toshinori, O.; Hideki, M.; Masato, W.; Hisashi, O.; Toshiya, W. *Thin Solid Membr.* **2006**, *502*, 108.
30. Li, Y.; Cai, W. P.; Duan, G.. T.; Cao, B. Q.; Sun, F. Q.; Lu, F. *J. Colloid Interface Sci.* **2005**, *287*, 634.
31. Park, S. H.; Lee, S. M.; Lim, H. S. *Appl. Mater. Interfaces* **2010**, *2*, 658.
32. Wang, S.; Li, Y. P.; Fei, X. L.; Sun, M. D.; Zhang, C. Q.; Li, Y. X.; Yang, Q. B.; Hong, X. *J. Colloid Interface Sci.* **2011**, *359*, 380.
33. Theron, S. A.; Yarin, A. L.; Zussman, E.; Kroll, E. *Polymer* **2005**, *46*, 2889.
34. Varesano, A.; Carletto, R. A.; Mazzuchetti, G. *J. Mater. Process. Technol.* **2009**, *209*, 5178.
35. Varabhas, J. S.; Chase, G. G.; Reneker, D. H. *Polymer* **2008**, *49*, 4226.
36. Yarin, A. L.; Zussman, E. *Polymer* **2004**, *45*, 2977.
37. Cassie, A. B. D.; Baxter, S. *Trans. Faraday Soc.* **1944**, *40*, 546.
38. Wenzel, R. *N Ind. Eng. Chem.* **1936**, *28*, 988.
39. Chen, W.; Fadeev, A. Y.; Hsieh, M. C.; Öner, D.; Youngblood, J.; McCarthy, T. J. *Langmuir* **1999**, *15*, 3395.